Inositol-Related Gene Knockouts Mimic Lithium's Effect on Mitochondrial Function

Lilach Toker[1,2,3], Yuly Bersudsky[2,3,4], Inbar Plaschkes[5], Vered Chalifa-Caspi[5], Gerald Berry[6], Dieder Moechars[7], RH Belmaker[2,3,4], Galila Agam[1,2,3]

[1]Department of Clinical Biochemistry and [2]Psychiatry Research Unit, [3]Faculty of Health Sciences, Ben-Gurion University of the Negev and [4]Mental Health Center, [5]National Institute for Biotechnology in the Negev (NIBN), Beer-Sheva, Israel; [6]Metabolism Program Division of Genetics, Children's Hospital Boston, Harvard Medical School, Boston, MA, USA; [7]Dieder Moechars, Johnson & Johnson Pharmaceutical Research and Development, Beerse, Belgium.

Corresponding Author:
Galila Agam, Ph.D.
Department of Clinical Biochemistry and
Psychiatry Research Unit
Faculty of Health Sciences
Ben-Gurion University of the Negev and
Mental Health Center
Beer-Sheva, Israel
Tel. 972-8-6401737
galila@bgu.ac.il

Summary

Bipolar-disorder, characterized by switches between depressive and manic mood, is treated by mood-stabilizers, lithium being one of them. Among hypotheses suggested, the inositol-depletion hypothesis proposes that lithium attenuates hyperactivation of phosphatidylinositol signaling linked to neurotransmission-related receptors.

Available for us are knockout-mice of two genes (*IMPA1* or *Slc5a3*) each encoding for a protein related to inositol metabolism. We previously characterized these mice as exhibiting lithium-like neurochemical and behavioral phenotype.

We performed a DNA-microarray study searching for pathways commonly affected by chronic lithium treatment and by the knockout of each of the genes. Here we show up-regulation of mitochondrial function in the three paradigms studied. To verify this result, interrelationship between treatment with lithium and rotenone, an inhibitor of mitochondrial function, was studied behaviorally. Lithium and rotenone counteracted each other's effects in two bipolar-related models. The results support the inositol-depletion hypothesis and suggest amelioration of aberrant mitochondrial function consequent to inositol-depletion.

Introduction

Bipolar-disorder is a multifactorial and polygenic psychiatric-illness characterized by switches between depressive and manic mood. Lithium-salts (Li) are among the main drugs used in its treatment. The mechanism of Li's mood-stabilization is not yet unraveled. Among hypotheses of Li's mechanism the inositol-depletion hypothesis proposes that Li acts by depletion of brain *myo*-inositol[1]. This is based on the uncompetitive inhibition of inositol monophosphatase-1 (IMPase-1), a key enzyme in the phosphatidylinositol (PI) cycle, by therapeutically-relevant Li levels resulting in decreased *myo*-inositol (inositol) and subsequent down-regulation of the PI-cycle[2]. Berridge[1] proposed that depletion of inositol leads to a decreased response to neurotransmission through this pathway. The inositol-depletion hypothesis is further supported by the observation that decrease in inositol is common to two other widely used mood stabilizers, valproic acid (VPA) and carbamazepine (CBZ)[3,4]. Williams et al.[5] demonstrated that the three mood-stabilizers inhibit the collapse of sensory neurons growth cones. This effect was reversed by addition of *myo*-inositol but not *scyllo*- or *epi*-inositol[6].

There are three sources of intracellular *myo*-inositol: 1. recycling in the PI cycle involving IMPase; 2. *de-novo* synthesis from glucose-6-phosphate *via* *myo*-inositol-1-phosphate synthase (MIP-synthase); 3. uptake from extracellular fluid through a sodium-*myo*-inositol cotransporter (SMIT) and the H^+-*myo*-inositol cotransporter (HMIT). MIP-synthase is inhibited by therapeutically-relevant VPA levels[4]. Chronic treatment with Li, VPA and CBZ decreased mRNA levels of SMIT1 in astrocytes[7] corroborating with the finding that SMIT1 mRNA levels were up-regulated in neutrophils of bipolar patients[8].

Li-treatment affects three behavioral paradigms in rodents: Li-pretreatment induces hypersensitivity to pilocarpine-induced seizures[9], chronic Li-treatment attenuates the amphetamine-induced hyperlocomotion model of mania[10] and decreases immobility-time in the forced-swim test (FST) model of depression[11,12].

Homozygote-knockout (KO) of each of the *IMPA1* or *Slc5a3* genes encoding IMPase-1 and SMIT1, respectively, is lethal but both KO offspring are rescued by supplementation of 2% *myo*-inositol in drinking water to pregnant and lactating dams[13,14]. Adult KO *IMPA1* mice exhibit ~50% reduction in brain IMPase activity with no difference in brain inositol levels[14] and are characterized by Li-like behavior: reduced immobility in the FST and hypersensitivity to pilocarpine[14]. Adult *Slc5a3* KO mice exhibit 60% reduction in brain inositol levels and also show Li-like reduced immobility in

the FST, hypersensitivity to pilocarpine-induced seizures[14] and attenuated response to amphetamine-induced hyperlocomotion (unpublished data).

Thus, there is behavioral and neurochemical similarity between Li-treated wildtype (WT) mice and mice harboring KO of either *IMPA1* or *Slc5a3*, both encoding for proteins involved in inositol metabolism and known to be affected by chronic Li-treatment. It is plausible to expect that prolonged intervention with a biological system would induce changes in the expression of genes related to biofunctions involved in the resulting phenotype. We assumed that biofunctions similarly affected by chronic Li-treatment and by KO of *IMPA1* or *Slc5a3* would be those involved in the common phenotype relevant to the mood-stabilizing effects of Li. Here we present a hypothesis-free micoarray study of frontal-cortex of untreated WT mice, Li-treated WT mice, *IMPA1* KO mice (IMPA1 KO) and *Slc5a3* KO mice (SMIT1 KO) behaviorally verified by a pharmacological intervention.

Results

Gene expression analysis

Since IMPA1 KO and SMIT1 KO mice were generated on different backgrounds the microarray analysis was carried out separately for each colony (further referred to as the SMIT1 colony or the IMPA1 colony). Three-way mixed model ANOVA of WT untreated and WT Li-treated mice from both colonies revealed that the major source of variation between the groups was the colony (Supplementary Fig. S2), supporting our *a priory* approach to perform the expression analysis separately for each colony.

IMPA1 colony: in the frontal cortex of both IMPA1 KO mice and Li-treated WT mice as compared with WT-untreated mice 193 genes were similarly differentially expressed (either up- or down-regulated) at a level of $p<0.05$. SMIT1 colony: in the frontal cortex of both SMIT1 KO mice and Li-treated WT mice as compared with WT-untreated mice 778 genes were similarly differentially expressed at a level of $p<0.05$. Hierarchical clustering of 4,643 genes differentially expressed by Li treatment or the KO in either of the colonies showed two major clusters of the samples corresponding to SMIT1 and IMPA1 colonies (Supplementary Fig. S3). Only one gene cluster consisting of 419 annotated genes showed similar expression pattern between the two colonies. Functional annotation of this gene cluster using DAVID software revealed that almost all functional annotations with FDR (false discovery rate)<0.05 are related to mitochondria,

specifically to respiratory function (Supplementary Fig. S4). Hierarchical clustering based on all differentially expressed genes in each colony separately (WT-Li *vs.* WT-untreated or KO *vs.* WT-untreated) revealed clustering of the KO samples with the Li-treatment samples (Fig. 1A,B).

The expression of seven genes was significantly changed ($p<0.05$) in the same direction (up- or down regulation) in KO mice and Li-treated WT mice in both colonies (IMPA1 and SMIT1), as compared to their respective WT-untreated littermates (Supplementary Table S1). Four of the genes – *Cox5a*, *Ndufab1*, *Ndufs7* and *Uqcrfs1* - take part in the oxidative phosphorylation (OxPhos) pathway and were all up-regulated compared to WT-untreated mice. Three of these genes, *Cox5a*, *Ndufs7* and *Ndufab1* have previously been indicated by at least two independent studies to be down-regulated in bipolar patients or genetically associated with bipolar disorder[15-18].

Analysis using DAVID software

For each colony genes with similar differential expression ($p<0.05$) in the frontal cortex of the KO mice and the Li-treated WT mice as compared to WT-untreated mice were uploaded onto the software. Out of the uploaded genes, 159 and 654 genes from the IMPA1 and SMIT1 colonies, respectively, were identified by the software and used for the analysis. In both colonies significantly enriched terms and significant KEGG pathways (Bonferoni corrected $p<0.05$, $FDR<0.05$) were composed of mitochondria-related genes (Supplementary Fig. S5A,B). KEGG pathways significantly enriched in both colonies were Parkinson's disease, Alzheimer's disease, Huntington's disease and OxPhos. Since the pathophysiology of the three diseases involves mitochondrial dysfunction[19], genes encoding for proteins of the electron transfer chain of OxPhos are included in their pathway. Hence, enrichment in OxPhos-related genes is identified by the software as enrichment in the pathways related to these three diseases. Indeed, almost all of the genes included in those pathways were part of the mitochondrial OxPhos chain. Within the OxPhos, the differentially expressed genes in both colonies belong to all complexes of the electron transfer chain except for complex II (Fig. 2A,B).

Analysis using the GSEA software

For both KOs the most significant gene-set found was "structural_constituent_of_ribosome" followed by various mitochondria-related gene-sets (Supplementary Table S2), all exhibiting up-regulation as compared to WT-untreated

mice. No significantly differentially expressed gene-sets were obtained in the Li-treatment groups, a result possibly related to the phenomenon that Li affects diseased individuals much more than healthy controls and that the behavioral effects of the drug are observed in challenged animals and not under baseline conditions.

Analysis using the IPA software

As seen in Fig. S5A, using the cut-offs of $p<0.05$, f.c.>1.1 and $p<0.035$, f.c>1.15 for the IMPA1 and SMIT1 colonies, respectively (as justified under the online available Methods), multiple biological functions were significantly affected both by Li treatment in the two colonies and by *IMPA1* or *Slc5a3* KO. The common significantly affected canonical pathways in the four groups (WT-Li treated mice from SMIT1 colony, WT-Li treated mice from IMPA1 colony, SMIT1 KO, IMPA1 KO) were OxPhos, mitochondrial dysfunction and ubiquinone biosynthesis, all related to mitochondria (Fig. S5B, Table 1).

Rotenone-induced behavioral effects

Based on our microarray results and previous reports of reduced mitochondrial function in bipolar patients[15,20] we hypothesized that chronic mild inhibition of OxPhos would induce a bipolar disorder-like behavioral phenotype and that such behavior would be ameliorated by chronic lithium treatment. Chronic treatment with rotenone, an OxPhos complex I inhibitor, is used to model Parkinson's disease. However, the doses shown to elicit Parkinson's-like effects are higher than those used in our study. No difference was found between rotenone-treated and untreated mice in weight, well being (monitored by the appearance of their fur and their home-cage behavior) or general motor function, confirming that rotenone concentration used did not affect the general condition of the animals. Mice exhibiting altered motor ability in either the hanging wire or the rotarod tests were excluded from further experiments.

Four treatment groups of mice were studied behaviorally in the FST and the amphetamine-induced hyperlocomotion paradigm: regular food + vehicle (Rf+vehicle), chronic lithium treatment + vehicle (Li+vehicle), regular food + chronic rotenone treatment (Rf+rot), chronic lithium treatment + chronic rotenone treatment (Li+rot). In the FST, as expected[11,12], lithium treatment exerted an antidepressant-like effect, reducing the immobility time as compared to both regular food groups, either rotenone-pretreated or vehicle-pretreated (Fig. 3). One-way ANOVA revealed a significant treatment effect ($F=8.6173$, $df=3$, $p<0.00006$). The effect of Li was stronger in vehicle-pretreated

(Rf+vehicle - 163 sec, Li+vehicle - 94 sec, Fisher's LSD post-hoc test, $p<0.0001$) than in rotenone-pretreated animals (Rf+rot – 170 sec, Li+rot – 132 sec, $p<0.03$). Chronic treatment with rotenone (Rf+rot) did not have a significant effect on the immobility time, though a consistent trend of increased immobility was observed in all four experiments. However, rotenone treatment significantly prevented the effect of lithium ($p<0.005$) (Fig. 3).

In the amphetamine-induced hyperlocomotion paradigm there was no difference among the groups prior to amphetamine administration. Rotenone augmented amphetamine-induced hyperlocomotion and Li treatment abolished this effect (Fig. 4). Two-way repeated measures ANOVA of the results following amphetamine administration indicated a significant treatment effect ($F=7.33$, $df=3$, $p<0.0005$) and timeXtreatment interaction ($F=2.77$, $df=15$, $p<0.0006$). Post-hoc analysis indicated that rotenone's augmentation of the effect of amphetamine was statistically significant (Fisher's LSD post-hoc test, $p<0.025$) and so was Li's effect to abolish rotenone's effect on amphetamine-induced hyperlocomotion (Fisher's LSD post-hoc test, $p<0.0002$) (Fig. 4).

Discussion

The first part of the present study was a hypothesis-free DNA microarray analysis looking for pathways underlying the mood-stabilizing effect of Li in mouse frontal cortex. We searched for shared gene expression patterns among Li-treated mice and mice harboring KO of either *IMPA1* or *Slc5a3*, both encoding proteins related to the PI cycle and shown to be affected by therapeutic levels of the drug. Our group has previously reported Li-like behavioral and neurochemical phenotypes exhibited by IMPA1 KO or SMIT1 KO mice[14]. The three different bioinformatics approaches used to analyze the microarray data consistently indicated involvement of mitochondrial function in the Li-like phenotype. This finding corroborates previous reports of down-regulation of mitochondria-related genes[16,17], mitochondrial dysfunction[20] and mitochondrial structural abnormalities[21] in bipolar patients. The results are also consistent with studies showing beneficial effects of mood stabilizers on mitochondrial function[22,23] and oxidative stress[24]. The striking similarity in biological functions and canonical pathways affected by Li-treatment and each of the KOs provides support for the inositol-depletion hypothesis and suggests that inositol metabolism is involved in Li's effect on OxPhos and mitochondrial function.

DNA microarray studies frequently seek confirmation using real-time PCR technique to verify the expression of specific genes found to be differentially expressed in the microarrays following a particular intervention. However, as discussed by Konradi et al.[25] in a recent review, the strength of transcriptome studies, such as microarrays, is the examination of the expression pattern of inter-related groups of genes. The likelihood for a concordant expression change in a group of genes with a similar function or location is much smaller than the likelihood to reach a significant change for an individual gene. Moreover, systemic analysis of gene expression obscures individual biological differences and smooths experimental bias, highlighting the main between-group differences. For example, the well established upregulation of BDNF and BCL-2 by chronic lithium treatment[26] is not robustly reflected in microarray studies[27]. There are at least two possible explanations for this phenomenon: 1. The use of stringent statistical tests such as correction for multiple testing and of relatively high cut-off values for the analysis of microarray data indeed decrease the number of "false-positive" differentially expressed genes, but at the cost of increased number of "false negatives", excluding genes with small but true fold of change and relatively high variance. 2. An organism is a complex network with multiple points of regulation. The activity of an enzyme or the level of a metabolite may be affected at the level of genetics, epigenetics, change in the levels of transcription factors, alternative splicing, existence of iRNAs, translation or degradation rate, activity of isoenzymes, etc. It is reasonable to assume that each individual has his own "network setup" which defines his personal response to environmental factors intervening with the network. Thus, particularly in multifactorial disorders, the expression level of a single gene would be a poor indicator of upstream causative factors or of the downstream consequences responsible for a final outcome. Indeed, several microarray studies were carried out to unravel the pathophysiology of bipolar disorder using different species, tissues, and mood-stabilizer treatment regimes[16,17,27], yet, among the reported candidate genes almost none replicated between the studies. On the other hand, quite a few of the studies indicated down-regulation of mitochondria-related genes in bipolar patients, with components of the electron transport chain in particular[16,17] and up-regulation of these biological components following chronic Li treatment[23].

Rather than confirming the microarray results by measuring mRNA levels of particular genes found to be differentially expressed, the second part of the study aimed to model the mitochondrial aspect of the pathophysiology of bipolar disorder and assess the

interaction between the effect of mild chronic treatment with rotenone and Li on bipolar-related behavioral paradigms in mice. As hypothesized, rotenone, a mitochondrial OxPhos complex I inhibitor, and Li exhibited counteracting effects in the FST model of depression and in the amphetamine-induced hyperlocomotion model of mania, supporting an interrelationship between Li's mood-stabilizing effect and mitochondrial function.

In the FST, rotenone treatment did not significantly affect the performance of the mice, possibly due to a ceiling effect, but it did significantly increase the immobility time of Li-treated mice. Namely, the antidepressant-like effect of Li on rotenone-treated mice was significantly lower than that on vehicle-treated mice. This is reminiscent of the situation in the clinics, where Li is regarded to be a better anti-manic and prophylactic agent than an antidepressant. It is possible that the pathophysiology accumulated prior to the commencement of Li treatment as modeled here by rotenone pretreatment can not be fully reversed by Li.

In the amphetamine-induced hyperlocomotion paradigm rotenone significantly augmented the effect of amphetamine, reminiscent of the increased sensitivity to psychostimulants of euthymic bipolar patients. Li treatment completely abolished amphetamine's effect both in vehicle-pretreated and rotenone-pretreated mice. Prior to amphetamine challenge no behavioral differences were observed among the groups, resembling euthymic patients or subjects with predisposition to bipolar disorder but yet asymptomatic.

Results obtained from behavioral paradigms should be interpreted cautiously since rodents commonly used in these studies are healthy. They do not possess the genetic or physiological deviations characterizing bipolar patients. Bipolar disorder-related behavioral animal models are based on a limited number of often poorly understood behavioral phenotypes and speculated susceptibility genes. The models are frequently strictly environmental, acute or subchronic (such as the FST, tail suspension test, psychostimulant-induced behaviors, dominant and submissive relationship) or based on specific gene knockouts, potentially involving undefined compensatory mechanisms. Thus, the observed effects of a drug (e.g. Li) in these models would most probably be more modest than (in the case of an acute model) or even unrelated to (as in the case of gene knockout models) those seen in patients. This might have caused the relatively small changes obtained in the microarray paradigm of the present study and is further supported by our behavioral results. As recently suggested by the members of a targeted expert meeting of the European College of Neuropsychopharmacology (ECNP)[28] an improved

model to investigate a multifactorial disorder would be one that resembles the progress of the illness in patients, e.g. mild but prolonged induction of pathophysiology assumed to be involved in the disorder. Such a model is expected to exhibit a disorder phenotype only following prolonged intervention and when additional risk-factors occur. We aimed to create such a model using chronic low doses of rotenone, modeling the reported mitochondrial dysfunction in bipolar patients[15,16,20]. This fits the concept that the disorder involves gradual decrease in mitochondrial function, with symptoms beginning only when a threshold is reached or when an event occurs which requires fully functional cells, making the subject more vulnerable to environmental factors targeting mitochondrial function. Amphetamine, a psychostimulant widely used to model mania was shown to inhibit respiratory chain activity, an effect reversed by Li or VPA treatment[23]. Although single-photon emission computed tomography (SPECT) imaging did not find increased striatal dopamine in euthymic bipolar patients in response to amphetamine as compared to healthy subjects the patients exhibited greater behavioral response to the psychosymulant[29], suggesting an increased sensitivity to the drug even during the euthymic stage. Interestingly, some but not all studies report that antidepressants induce an inhibitory effect on mitochondrial complexes and a decrease in mitochondrial membrane potential ($\Delta\Psi m$)[30]. It is tempting to speculate that these effects underly antidepressant-induced mania in bipolar patients.

Mitochondria are the main source of cellular energy obtained as adenosine triphosphate (ATP) through the OxPhos pathway. However, energy homeostasis is only one of several essential processes related to mitochondrial function. Other well recognized processes are apoptosis[31] and calcium buffering and homeostasis[32,33]. IP_3, one of the two PI cycle-related second messengers, binds to its receptor (IP_3R) located on the endoplastic reticulum (ER) membrane, resulting in Ca^{2+} secretion. Previous studies demonstrated proximity of IP_3R to mitochondria and rapid increase in mitochondrial Ca^{2+} levels following IP_3-induced Ca^{2+} release[32]. Rapid elevation of mitochondrial Ca^{2+} induces opening of the mitochondrial permeability transition pore (MPT) in the inner membrane[34], which might result in decreased mitochondrial membrane potential, decreased mitochondrial function and increased production of reactive oxygen species (ROS)[34,35]. Kubota et al.[36] demonstrated that inhibition of cyclophilin D (CypD), a protein known to be part of the MPT, improved the abnormal behavior of mitochondrial DNA polymerase (Polg1) KO mice, suggested by the authors as an animal model of bipolar disorder[36]. Expression of *PPIF*, the gene encoding for the CypD protein, was found to be

down-regulated both in the brains of bipolar patients and in the *Polg1* mutant mice, possibly due to a compensatory mechanism[36].

Over the last decade, evidence accumulated regarding a reciprocal relationship between mitochondria and autophagy[37], a cellular pathway required for proper lysosomal degradation of misfolded proteins and their aggregates, long-lived proteins, damaged organelles and pathogens. Several studies reported that the three mood-stabilizers Li, VPA and CBZ, all known to reduce inositol levels[5] upregulate autophagy[38,39]. Increased autophagy was also achieved by treatment with the specific IMPase inhibitor L-690,330 but not the GSK-3β inhibitor SB216763[38]. Furthermore, the pro-autophagic effect of Li was reversed by addition of *myo*-inositol[38], indicating the involvement of inositol-depletion in the effect of the three mood stabilizers on autophagy. Interestingly, Parkinson's disease, Alzheimer's disease, Huntington's disease and Amyotrophic Lateral Sclerosis (ALS), all neurodegenerative diseases which exhibit well established involvement of mitochondrial dysfunction[19], are also related to aberrant autophagy[40], and were suggested to benefit from Li treatment[41]. Recent studies reported that cells lacking mitochondrial DNA (mtDNA) or functional OxPhos complexes display impaired autophagy[42] and that autophagy is required for the maintenance of mtDNA under nitrogen starvation in yeast[43]. Thus, it is possible that mitochondrial function and autophagy are interconnected, with alterations in one of the processes initiating a vicious cycle of accumulating dysfunctions. Our present findings that inositol-depletion possibly underlies Li's effect on mitochondrial function raise the question whether inositol-depletion directly affects only one of the two processes, which, in turn, projects on the function of the other, or whether an independent effect is exerted on the two interconnected pathways. Intriguingly, rapamycin, an autophagy activator, was reported to protect against rotenone-induced apoptosis *via* induction of autophagy[44]. A similar effect of protection against rotenone-induced apoptosis was obtained by Li or VPA treatment[24], an effect interpreted by the authors as related to the beneficial effect of the two mood-stabilizers on oxidative stress and OxPhos.

In summary, this is the first report of a whole genome gene expression study carried concomitantly in Li-treated mice and in mice exhibiting Li-like behavior induced by KO of one of two genes, both encoding proteins belonging to a particular pathway and known to be affected by Li. We replicated results of previous studies both at the level of single genes and at the level of systems biology, giving credence to our experimental design. Based on our microarray findings and using a pharmacological intervention we

induced bipolar-like behavior, reversed by Li treatment. Our results support the inositol-depletion hypothesis of Li's mechanism of action and suggest that mitochondrial dysfunction might be involved in the pathophysiology of bipolar disorder ameliorated by mood stabilizers *via* their effect on inositol metabolism.

Methods Summary

Fig. S1 (supplementary information) presents a schematic layout of the study.

Microarrays

Each of the SMIT1 and IMPA1 KO mice were maintained in a separate colony by breeding heterozygote males and females. Chronic lithium treatment was carried out as previously described[12]. Serum Li levels were 0.9 mmol/L ± 0.4 (SD). In each of the SMIT1 and IMPA1 colonies three groups (4 mice/group) were examined: WT-untreated, WT-Li treated and KO (IMPA1 or SMIT1). Extracted RNA was hybridized to Affimetrix Mouse Gene 1.0 ST chips. Initial data analysis was carried out using the Partek® and SpotFire software. Three-way mixed-model ANOVA was used to analyze the difference between the colonies regarding Li's effect. Subsequently, two-way mixed-model ANOVA was carried out separately in each colony to assess the effect of Li-treatment and of the KO of each of the genes. Differentially-expressed genes were defined as those having $p<0.05$ compared to WT-untreated mice. For clustering analysis, signals were batch-corrected using Partek®. Genes showing differential expression in either Li-treated animals or KO animals were included in the analysis. The Hierarchical Clustering tool of the SpotFire software was used to create dendrogram of z-score-transformed signals. Bioinformatics analysis was carried out using the DAVID, GSEA and IPA software.

Behavior

ICR mice were injected subcutaneously once daily with rotenone (0.5 mg/kg) or vehicle for 4 weeks. Chronic Li regime was applied during the last two weeks of injections. After four weeks all animals were evaluated for motor function by the hanging wire and the rotarod tests a day prior to the behavioral paradigms. The FST and amphetamine-induced hyperlocomotion were performed on consecutive days. Effect of treatment on behavior in the FST was analyzed using ANOVA followed by Fisher's LSD post-hoc test. Repeated-measures ANOVA followed by Fisher's LSD post-hoc test was used to assess the effect on amphetamine-induced hyperlocomotion.

References

1 Berridge, M. J., Downes, C. P., and Hanley, M. R., Neural and developmental actions of lithium: a unifying hypothesis. *Cell* **59** (3), 411 (1989).

2 Hallcher, L. M. and Sherman, W. R., The effects of lithium ion and other agents on the activity of myo-inositol-1-phosphatase from bovine brain. *J Biol Chem* **255** (22), 10896 (1980).

3 O'Donnell, T. et al., Chronic lithium and sodium valproate both decrease the concentration of myo-inositol and increase the concentration of inositol monophosphates in rat brain. *Brain Res* **880** (1-2), 84 (2000).

4 Shaltiel, G. et al., Valproate decreases inositol biosynthesis. *Biol Psychiatry* **56** (11), 868 (2004).

5 Williams, R. S., Cheng, L., Mudge, A. W., and Harwood, A. J., A common mechanism of action for three mood-stabilizing drugs. *Nature* **417** (6886), 292 (2002).

6 Shaltiel, G. et al., Specificity of mood stabilizer action on neuronal growth cones. *Bipolar Disord* **9** (3), 281 (2007).

7 Lubrich, B. and van Calker, D., Inhibition of the high affinity myo-inositol transport system: a common mechanism of action of antibipolar drugs? *Neuropsychopharmacology* **21** (4), 519 (1999).

8 Willmroth, F. et al., Sodium-myo-inositol co-transporter (SMIT-1) mRNA is increased in neutrophils of patients with bipolar 1 disorder and down-regulated under treatment with mood stabilizers. *Int J Neuropsychopharmacol* **10** (1), 63 (2007).

9 Belmaker, R. H. and Bersudsky, Y., Lithium-pilocarpine seizures as a model for lithium action in mania. *Neurosci Biobehav Rev* **31** (6), 843 (2007).

10 Einat, H. et al., The role of the extracellular signal-regulated kinase signaling pathway in mood modulation. *J Neurosci* **23** (19), 7311 (2003).

11 Bersudsky, Y., Shaldubina, A., and Belmaker, R. H., Lithium's effect in forced-swim test is blood level dependent but not dependent on weight loss. *Behav Pharmacol* **18** (1), 77 (2007).

12 O'Brien, W. T. et al., Glycogen synthase kinase-3beta haploinsufficiency mimics the behavioral and molecular effects of lithium. *J Neurosci* **24** (30), 6791 (2004).

13 Berry, G. T. et al., Loss of murine Na+/myo-inositol cotransporter leads to brain myo-inositol depletion and central apnea. *J Biol Chem* **278** (20), 18297 (2003).

14 Agam, G. et al., Knockout mice in understanding the mechanism of action of lithium. *Biochem Soc Trans* **37** (Pt 5), 1121 (2009).

15 Washizuka, S. et al., Expression of mitochondria-related genes in lymphoblastoid cells from patients with bipolar disorder. *Bipolar Disord* **7** (2), 146 (2005).

16 Sun, X., Wang, J. F., Tseng, M., and Young, L. T., Downregulation in components of the mitochondrial electron transport chain in the postmortem frontal cortex of subjects with bipolar disorder. *J Psychiatry Neurosci* **31** (3), 189 (2006).

17 Andreazza, A. C., Shao, L., Wang, J. F., and Young, L. T., Mitochondrial complex I activity and oxidative damage to mitochondrial proteins in the prefrontal cortex of patients with bipolar disorder. *Arch Gen Psychiatry* **67** (4), 360 (2010).

18 Konradi, C. et al., Molecular evidence for mitochondrial dysfunction in bipolar disorder. *Arch Gen Psychiatry* **61** (3), 300 (2004).

19 WTCCC, Genome-wide association study of 14,000 cases of seven common diseases and 3,000 shared controls. *Nature* **447** (7145), 661 (2007).

20 Stork, C. and Renshaw, P. F., Mitochondrial dysfunction in bipolar disorder: evidence from magnetic resonance spectroscopy research. *Mol Psychiatry* **10** (10), 900 (2005).

21 Cataldo, A. M. et al., Abnormalities in mitochondrial structure in cells from patients with bipolar disorder. *Am J Pathol* **177** (2), 575 (2010).

22 Maurer, I. C., Schippel, P., and Volz, H. P., Lithium-induced enhancement of mitochondrial oxidative phosphorylation in human brain tissue. *Bipolar Disord* **11** (5), 515 (2009).

23 Valvassori, S. S. et al., Effects of mood stabilizers on mitochondrial respiratory chain activity in brain of rats treated with d-amphetamine. *J Psychiatr Res* **44** (14), 903 (2010).

24 Lai, J. S., Zhao, C., Warsh, J. J., and Li, P. P., Cytoprotection by lithium and valproate varies between cell types and cellular stresses. *Eur J Pharmacol* **539** (1-2), 18 (2006).

25 Konradi, C., Sillivan, S. E., and Clay, H. B., Mitochondria, oligodendrocytes and inflammation in bipolar disorder: Evidence from transcriptome studies points to intriguing parallels with multiple sclerosis. *Neurobiol Dis* (2011).

26 Machado-Vieira, R., Manji, H. K., and Zarate, C. A., Jr., The role of lithium in the treatment of bipolar disorder: convergent evidence for neurotrophic effects as a unifying hypothesis. *Bipolar Disord* **11 Suppl 2**, 92 (2009).

27 McQuillin, A., Rizig, M., and Gurling, H. M., A microarray gene expression study of the molecular pharmacology of lithium carbonate on mouse brain

mRNA to understand the neurobiology of mood stabilization and treatment of bipolar affective disorder. *Pharmacogenet Genomics* **17** (8), 605 (2007).

28 Chetcuti, A., Adams, L. J., Mitchell, P. B., and Schofield, P. R., Microarray gene expression profiling of mouse brain mRNA in a model of lithium treatment. *Psychiatr Genet* **18** (2), 64 (2008).

29 Kas, M. J. et al., Advances in multidisciplinary and cross-species approaches to examine the neurobiology of psychiatric disorders. *Eur Neuropsychopharmacol* **21** (7), 532 (2011).

30 Anand, A. et al., Brain SPECT imaging of amphetamine-induced dopamine release in euthymic bipolar disorder patients. *Am J Psychiatry* **157** (7), 1108 (2000).

31 Hroudova, J. and Fisar, Z., Connectivity between mitochondrial functions and psychiatric disorders. *Psychiatry Clin Neurosci* **65** (2), 130 (2011).

32 Wang, X., The expanding role of mitochondria in apoptosis. *Genes Dev* **15** (22), 2922 (2001).

33 Rizzuto, R. et al., Close contacts with the endoplasmic reticulum as determinants of mitochondrial Ca2+ responses. *Science* **280** (5370), 1763 (1998).

34 Gunter, T. E. and Gunter, K. K., Uptake of calcium by mitochondria: transport and possible function. *IUBMB Life* **52** (3-5), 197 (2001).

35 Crompton, M. and Costi, A., Kinetic evidence for a heart mitochondrial pore activated by Ca2+, inorganic phosphate and oxidative stress. A potential mechanism for mitochondrial dysfunction during cellular Ca2+ overload. *Eur J Biochem* **178** (2), 489 (1988).

36 Pivovarova, N. B. and Andrews, S. B., Calcium-dependent mitochondrial function and dysfunction in neurons. *FEBS J* **277** (18), 3622 (2010).

37 Kubota, M. et al., Therapeutic implications of down-regulation of cyclophilin D in bipolar disorder. *Int J Neuropsychopharmacol* **13** (10), 1355 (2010).

38 Hailey, D. W. et al., Mitochondria supply membranes for autophagosome biogenesis during starvation. *Cell* **141** (4), 656 (2010).

39 Zhang, H. et al., Oxidative stress induces parallel autophagy and mitochondria dysfunction in human glioma U251 cells. *Toxicol Sci* **110** (2), 376 (2009).

40 Okamoto, K., Mitochondria breathe for autophagy. *EMBO J* **30** (11), 2095 (2011).

41 Elmore, S. P., Qian, T., Grissom, S. F., and Lemasters, J. J., The mitochondrial permeability transition initiates autophagy in rat hepatocytes. *FASEB J* **15** (12), 2286 (2001).

[42] Sarkar, S. et al., Lithium induces autophagy by inhibiting inositol monophosphatase. *J Cell Biol* **170** (7), 1101 (2005).

[43] Hidvegi, T. et al., An autophagy-enhancing drug promotes degradation of mutant alpha1-antitrypsin Z and reduces hepatic fibrosis. *Science* **329** (5988), 229 (2010).

[44] Fu, J. et al., Autophagy induced by valproic acid is associated with oxidative stress in glioma cell lines. *Neuro Oncol* **12** (4), 328 (2010).

[45] Su, B. et al., Abnormal mitochondrial dynamics and neurodegenerative diseases. *Biochim Biophys Acta* **1802** (1), 135 (2010).

[46] Wong, E. and Cuervo, A. M., Autophagy gone awry in neurodegenerative diseases. *Nat Neurosci* **13** (7), 805 (2010).

[47] Chiu, C. T. and Chuang, D. M., Molecular actions and therapeutic potential of lithium in preclinical and clinical studies of CNS disorders. *Pharmacol Ther* **128** (2), 281 (2010).

[48] Graef, M. and Nunnari, J., Mitochondria regulate autophagy by conserved signalling pathways. *EMBO J* **30** (11), 2101 (2011).

[49] Suzuki, S. W., Onodera, J., and Ohsumi, Y., Starvation induced cell death in autophagy-defective yeast mutants is caused by mitochondria dysfunction. *PLoS One* **6** (2), e17412 (2011).

[50] Pan, T. et al., Rapamycin protects against rotenone-induced apoptosis through autophagy induction. *Neuroscience* **164** (2), 541 (2009).

Table 1. Canonical pathways found by the IPA software to be significantly affected in the frontal cortex of Li-treated WT mice and *IMPA1* or *SMIT1* KO mice

Canonical Pathway	p-value IMPA1 KO	Ratio* IMPA1 KO	p-value IMPA_Li	Ratio IMPA1_Li	p-value SMIT1 KO	Ratio SMIT1 KO	p-value SMIT_Li	Ratio SMIT_Li
OxPhos	6.77E-06	17/166	2.43E-04	13/166	5.14E-03	10/166	3.86E-06	19/166
Mitochondrial dysfunction	8.17E-05	14/125	2.25E-02	8/125	1.26E-04	12/125	3.89E-06	17/125
Ubiquinone biosynthesis	2.33E-04	10/119	1.48E-03	8/119	1.41E-02	7/119	2.12E-03	9/119

Gene expression data of the SMIT1 KO mice, Li-treated WT mice from the SMIT1 colony (SMIT_Li), IMPA1 KO mice and Li-treated WT mice from the IMPA1 colony (IMPA_Li) was subjected to IPA canonical pathway analysis. Genes from the uploaded data sets that met the cut-offs ($p<0.05$, f.c.>1.1 and $p<0.035$, f.c.>1.15 for the IMPA1 and the SMIT1 colonies, respectively) and that were associated with a canonical pathway in the Ingenuity Knowledge Base were considered for the analysis.

* Ratio indicates the number of genes from the data set that map to the pathway divided by the total number of genes that map to the canonical pathway. Fisher's exact test was used to calculate the p-value determining the probability that the association between the genes in the dataset and the canonical pathway is explained by chance only.

Figure legends

Hierarchal clustering of differentially-expressed genes show clustering of Li-treated mice with both SMIT1 KO (A) and IMPA1 KO (B) mice

Two-way ANOVA was carried out separately in each colony to reveal genes whose expression was affected by Li treatment or KO of either *IMPA1* or *Slc5a3* as compared to WT-untreated mice. Heatmaps and dendrograms were created separately for each colony. Genes differentially expressed ($p<0.05$) in either KO mice or in Li-treated mice (2,813 and 2,136 genes in SMIT1 **(A)** and IMPA1 **(B)** colony, respectively) were used for the analysis. Z-score calculation and cluster analysis were carried out for each colony separately. Colored bars represent the type of mice (yellow – WT-untreated, pink – KO, grey – WT-Li treated). Each raw represents an individual gene and each column a mouse. Green=negative Z-score; Red=positive Z-score.

Fig. 2: Localization of the commonly differentially expressed genes among the different complexes of the respiratory chain

The OxPhos pathway is depicted. Asterisks denote genes with similar differential expression in KO mice and Li-treated WT mice compared to WT-untreated mice in the SMIT1 colony **(A)** and the IMPA1 colony **(B)**. In both colonies the commonly differentially expressed genes were located in all the respiratory complexes except for complex II.

Fig. 3: Prevention of Li's antidepressant-like effect in the FST by chronic rotenone treatment

Animals were placed for 6 minutes in a glass cylinder filled with water at a temperature of 24^0C such that the mouse could not touch the bottom or climb out of the cylinder. The duration of immobility was monitored during the last four min of the six min test.

Results are means +/- S.E.M.

Rf – regular food; Li – lithium-supplemented regular food; vehicle – 0.5% DMSO in saline; rot – rotenone. ANOVA revealed a significant treatment effect ($F=8.6173$, $df=3$, $p<0.00006$). Rotenone did not affect the immobility time; lithium significantly reduced the immobility time. Rotenone prevented the effect of lithium. Fisher's LSD post-hoc test: * $p<0.05$ compared to Li+vehicle, # $p<0.05$ compared to Li+rot.

Fig. 4: Prevention of rotenone-augmented amphetamine-induced hyperlocomotion by Li-treatment

Mice were placed individually into monitor boxes and their behavior was digitally recorder for 30 min (habituation period). After 30 min mice were injected 1.5 mg/kg d-amphetamine i.p. and digitally recorded for one hour. Distance moved was analyzed using the Ethovision system.

Results are means +/- s.e.m.

No difference was found among the groups prior to amphetamine injection. Repeated measures ANOVA of the results following amphetamine treatment revealed a significant treatment effect ($F=7.33$, $df=3$, $p<0.0005$) and timeXtreatment interaction ($F=2.77$, $df=15$, $p<0.0006$). Rotenone significantly augmented the effect of amphetamine (Fisher's LSD post-hoc test, $p<0.025$). Li treatment prevented the effect of rotenone on amphetamine-induced hyperactivity (Fisher's LSD post-hoc test $p<0.0002$).

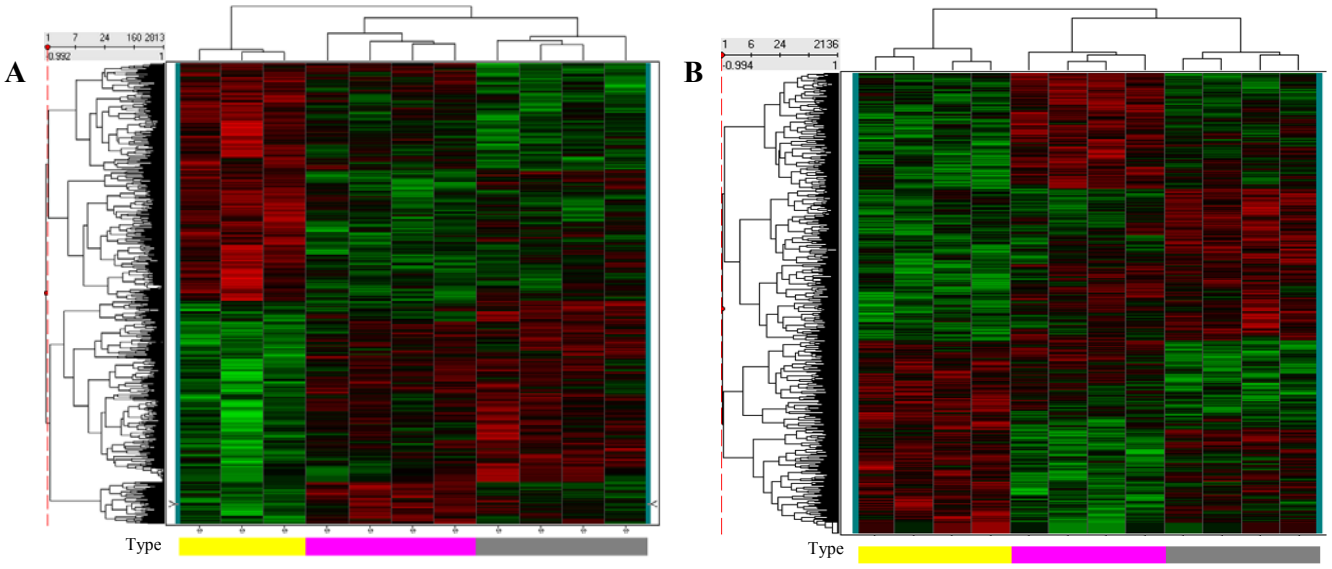

Fig. 1: Hierarchal clustering of differentially-expressed genes show clustering of Li-treated mice with both SMIT1 KO (A) and IMPA1 KO mice (B)

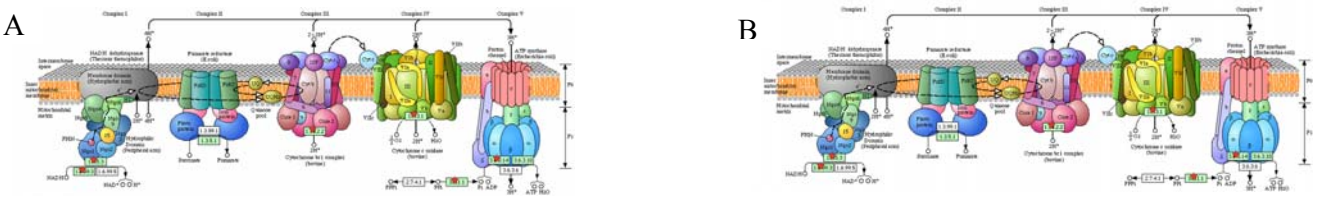

Fig. 2: Localization of the commonly differentially expressed genes among the different complexes of the respiratory chain.

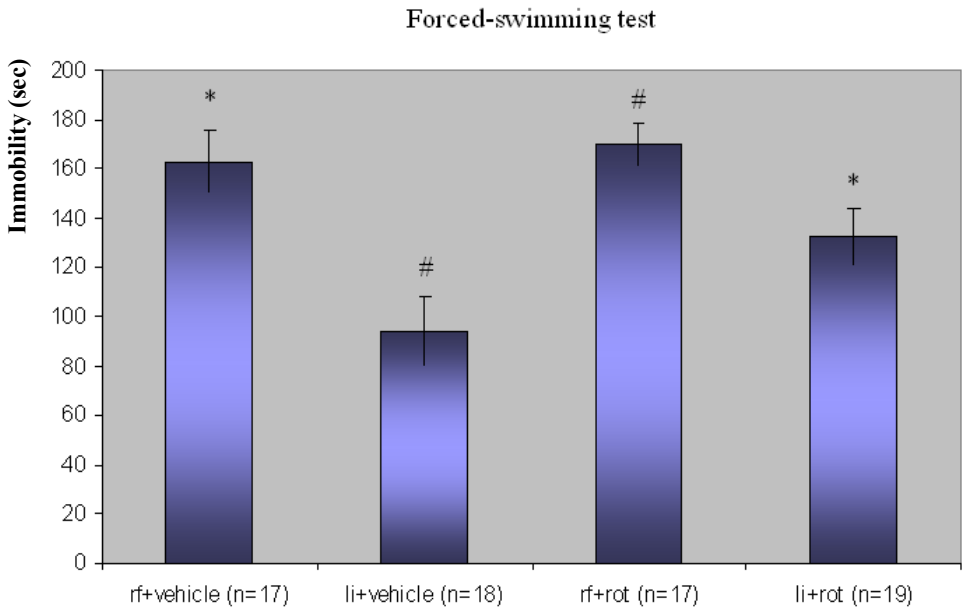

Fig. 3: Prevention of Li's antidepressant-like effect in the FST by chronic rotenone treatment

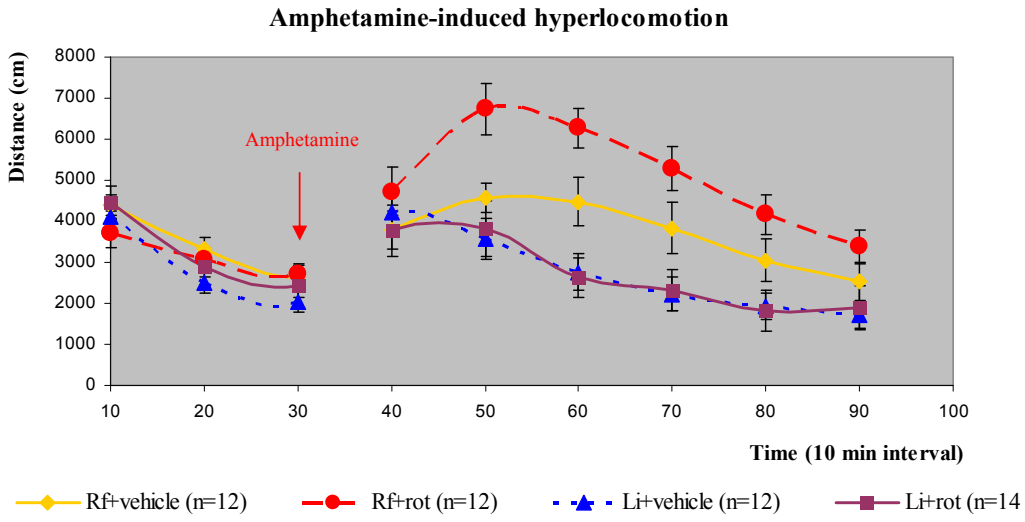

Fig. 4: Prevention of rotenone-augmented amphetamine-induced hyperlocomotion by Li-treatment

Methods

Animals

Male, eight weeks old mice were used in all the experiments. Animals were maintained on a 12h/12h light/dark cycle (lights on between 8:00 a.m and 8:00 p.m.) with *ad libitum* access to food and water. All tests were performed during the light phase of the cycle between 9:00 am and 7:00 pm. SMIT1 and IMPA1 KO mice were originally generated as previously described[13,45]. Each KO is maintained in a separate colony in our animal-care facility by breeding heterozygote males and females. *Myo*-inositol supplementation in drinking water to pregnant and lactating dams is used to rescue the KO mice. Genotyping was carried out as previously described[45,46]. ICR mice (Harlan, Israel) were allowed to acclimatize to the new environment for one week before treatment initiation. All experiments were approved by the Ben-Gurion University animal experimentation ethics committee.

Chronic lithium treatment

Chronic lithium treatment was carried out as previously described[12]. Animals were weighed every two days during the treatment period. The measured serum Li levels following this treatment regime were 0.89 mmol/L ± 0.43 (s.d.).

RNA extraction

Total RNA was extracted from frontal cortex specimens using TRI reagent (Sigma-Aldrich, St. Louis, MO) followed by purification using the RNeasy kit (Qiagen, Germantown, MD). RNA concentration was determined spectrophotometrically (GeneQuant, Pharmacia).

DNA Microarray gene expression

Since IMPA1 KO and SMIT1 KO mice were generated on different backgrounds (C57BL/129X1/Svj for SMIT1 and C57BL6/129Sv/EvBrd for IMPA1), the microarray analysis was carried out separately for each colony. In each colony three groups with four animals per group were examined: WT-untreated, WT-Li treated and KO (IMPA1 or SMIT1). Extracted RNA was hybridized to Affimetrix Mouse Gene 1.0 ST chips. Hybridization was carried out at the DNA microarrays and DNA sequencing Laboratory of the National Institute for Biotechnology in the Negev, Beer-Sheva, Israel, affiliated to our university.

Statistical analysis of the DNA microarrays

Initial data analysis was supervised by V.C-C. from the Bioinformatics Core Facility, National Institute for Biotechnology in the Negev, using the Partek® and SpotFire software. Briefly, signals were $\log_2$ transformed and preprocessed using the robust multi-chip average (RMA) method[47]. Principal component analysis (PCA) was performed for each colony separately. In both cases, a batch effect was found, which was balanced with regard to the biological groups. Probe sets with $\log_2$-transformed signals below a value of five in all samples were considered as "noise" and excluded from further analysis. Initially, three-way mixed model ANOVA was used to analyze the difference between the colonies regarding the effect of Li. The following effects were included in the analysis: WT-Li *vs.* WT-untreated as the biological effect, colony (IMPA1 or SMIT1) and batch as random effects (batch effect included in the colony). Subsequently, two-way mixed model ANOVA was carried out separately in each colony to assess the effect of Li treatment and of the KO of each of the genes. The following effects were used in the analysis: type (WT-untreated, WT-Li treated, KO) as the biological effect and batch as the random effect. Differentially expressed genes were defined as those having $p<0.05$ compared to WT-untreated mice.

For clustering analysis, signals were batch-corrected using Partek® software. Genes showing differential expression in either Li-treated animals or KO animals were included in the analysis. The Hierarchical Clustering tool of SpotFire software was used to create heatmap and dendrogram of z-score transformed signals.

Network and pathway analysis

The Functional Annotation Tool in DAVID 6.7 (the Database for Annotation, Visualization and Integrated Discovery) bioinformatics software was used according to the publisher's recommendations[48] for enrichment analysis of the genes differentially expressed in the same direction in the KO mice and Li-treated WT mice compared to WT-untreated mice in each colony.

The raw data of the microarray results was uploaded onto the Gene Set Enrichment Analysis (GSEA) V2.5 software[49], a computational method that determines whether an *a priori* defined set of genes ("gene-sets") shows statistically significant concordant differences between two biological states. GSEA calculates an enrichment score (ES) for a given gene-set using a ranked list of genes. The rank represents the correlation between the expression of the gene and the phenotype. ES is calculated by walking down the ranked list of genes, increasing a running-sum statistic when a gene is

in the gene-set and decreasing it when it is not. Further, the software infers the statistical significance of each ES against background ES distribution calculated by randomly shuffling the labels on the samples (phenotype permutation) or by creating random gene-sets matching the actual size of a particular gene-set (gene_set permutation). Given the relatively small sample size in our study we used the setup of 1000 gene-set permutations for analysis and a false discovery rate (FDR) cut-off of q-value<0.05 in order to identify differentially expressed sets of genes, as advised by the software team (http://www.broadinstitute.org/gsea/doc/GSEAUserGuideFrame.html), using an *a priory* defined sets of genes (GO gene-set collection "c5.all.v2.5.symbols").

Data was further analyzed through the use of IPA (Ingenuity® Systems, www.ingenuity.com) to identify pathways and functions affected by *IMPA1* KO, *Slc5a3* KO and Li treatment. In order to reach the recommended number of genes to be used in the analysis the cut-offs for p-value and fold of change (f.c.) were set to $p<0.05$, $|f.c.|>1.1$ and $p<0.035$, $|f.c|>1.15$ for the IMPA1 and the SMIT1 colonies, respectively. The functional analysis identifies the biological functions and/or diseases that were most significant to the data set. Genes from the uploaded dataset that met the cut-offs mentioned above and were associated with biological functions and/or diseases in the Ingenuity Knowledge Base were considered for the analysis. Right-tailed Fisher's exact test was used to calculate a p-value determining the probability that each biological function and/or disease assigned to that data set is due to chance only.

Canonical pathway analysis was used to identify the pathways in the IPA library of canonical pathways that were most significant to the uploaded data set. Genes from the data set that met the above mentioned cut-offs and were associated with a canonical pathway in the Ingenuity Knowledge Base were considered for the analysis. The significance of the association between the data set and the canonical pathway was measured in two ways: 1) A ratio of the number of genes from the data set that map to the pathway, divided by the total number of molecules that map to the canonical pathway. 2) Fisher's exact test was used to calculate a p-value determining the probability that the association between the genes in the dataset and the canonical pathway is explained by chance only.

Drugs

Rotenone (Sigma-Aldrich, St. Louis, MO) was dissolved in 0.5% DMSO in saline and injected subcutaneously (s.c.), 0.5 mg/kg and 5 ml/kg. d-Amphetamine (Sigma-

Aldrich, Gillinfhuam, UK) was dissolved in saline and injected intraperitonealy (i.p), 1.5 mg/kg and 10 ml/kg.

Rotenone treatment

ICR mice were injected once daily s.c. with rotenone or vehicle for 4 weeks. After two weeks of injections each of the groups was divided into two subgroups of Li treatment and regular food as described above for lithium treatment. All animals were daily weighed and their general well being was assessed by examination of their fur, general appearance and home-cage behavior. After four weeks of treatment all animals were evaluated for motor function by the hanging wire and rotarod tests a day prior to the behavioral paradigms. Animals with aberrant performance in either of the tests were excluded from further experiments. The FST and amphetamine-induced hyperlocomotion were performed on consecutive days. Four experiments were carried out, each including four treatment groups with 5 mice/group.

Hanging wire test

Each animal was placed on a metal grid which was gently shacked to cause grabbing reflex and slowly turned upside down. Latency to fall was counted during a session of one minute.

Rotarod test

Animals were subjected to a series of one minute sessions separated by 10 minutes on the rotarod apparatus (ROTA-ROD/RS, Letica Scientific Instruments, Panlab, Barcelona, Spain) using the following protocol: 0 rpm, 4 rpm, three sessions of accelerating 4 rpm to 40 rpm (two training sessions followed by the test session). Latency to fall was counted for each session.

[51] Cryns, K. et al., IMPA1 is essential for embryonic development and lithium-like pilocarpine sensitivity. *Neuropsychopharmacology* **33** (3), 674 (2008).

[52] Bersudsky, Y. et al., Homozygote inositol transporter knockout mice show a lithium-like phenotype. *Bipolar Disord* **10** (4), 453 (2008).

[53] Irizarry, R. A. et al., Exploration, normalization, and summaries of high density oligonucleotide array probe level data. *Biostatistics* **4** (2), 249 (2003).

[54] Huang, D, W., Sherman, B. T., and Lempicki, R. A., Systematic and integrative analysis of large gene lists using DAVID bioinformatics resources. *Nat Protoc* **4** (1), 44 (2009).

[55] Subramanian, A. et al., Gene set enrichment analysis: a knowledge-based approach for interpreting genome-wide expression profiles. *Proc Natl Acad Sci U S A* **102** (43), 15545 (2005).

Supplementary Information is linked to the online version of the paper at www.nature.com/nature

Acknowledgement

We wish to thank Dr. Micha Volokita from the National Institute for Biotechnology in the Negev (NIBN), Beer-Sheva, Israel, and his stuff for carrying out the hybridization with the Affimetrix chips, the readout of the raw data and the initial quality control assessment of the microarrays.

Author contributions

L.T. carried out all the experiments and the bioinformatics analyses and wrote the paper. Y.B. supervised the behavioral experiments. I.P. and V.C-C supervised the statistical analysis of the raw microarrays data. G.B. created the SMIT1 KO mice. D.M. created the IMPA1 KO mice. R.H.B. and G.A. initiated the study, supervised it and intensively contributed to the final version of the manuscript.

Author information

Reprints and permissions information is available at www.nature.com/reprints.

Neither of the authors have competing financial interests.

Correspondance and requests for materials should be addressed to galila@bgu.ac.il.

Supplementary Information

Supplementary Table S1: Genes with common expression change in IMPA1 KO, SMIT1 KO and Li treated mice

Gene symbol	Entrez Gene Name	p-value SMIT KO	Fold of change SMIT KO	p-value SMIT_ Li	Fold of change SMIT_ Li	p-value IMPA KO	Fold of change IMPA KO	p-value IMPA_ Li	Fold of change IMPA_ Li
Cox5a *	Cytochrome c oxidase, subunit Va	0.004	1.27	0.007	1.22	0.02	1.16	0.016	1.18
Gaa	glucosidase, alpha, acid	0.03	-1.32	0.01	-1.4	0.015	-1.2	0.036	-1.16
Gemin4	gem (nuclear organelle) associated protein 4	0.016	-1.18	0.003	-1.25	0.013	-1.12	0.006	-1.15
*Ndufab1**	NADH dehydrogenase (ubiquinone) 1, alpha/beta subcomplex,	0.019	1.16	0.005	1.2	0.01	1.2	0.03	1.14
*Ndufs7**	NADH dehydrogenase (ubiquinone) Fe-S protein 7	0.042	1.2	0.02	1.22	0.014	1.15	0.02	1.13
Rc3h1	RING CCCH (C3H) domains 1	0.02	-1.11	0.0005	-1.22	0.04	-1.08	0.02	-1.1
Uqcrfs1	ubiquinol-cytochrome c reductase, Rieske iron-sulfur polypeptide 1	0.03	1.15	0.0008	1.3	0.009	1.2	0.04	1.14

Seven genes were found to be similarly differentially expressed in SMIT1 KO mice, Li-treated WT mice from the SMIT1 colony (SMIT_Li), IMPA1 KO mice and Li-treated WT mice from the IMPA1 colony (IMPA_Li) as compare to their WT-untreated littermates. Four of these genes participate in the oxidative phosphorylation pathway, all up-regulated compared to WT untreated mice. Asterisk indicates genes previously reported to be down-regulated in or genetically associated with bipolar disorder in at least two independent studies.

Supplementary Table S2: Gene_sets showing significant difference between KO mice and WT-untreated mice

***IMPA1* KO mice *vs.* WT-untreated mice**				
NAME	Size*	FDR q-value**	p-value	NES***
STRUCTURAL CONSTITUENT OF RIBOSOME	77	2.14E-03	< 1.00E-04	2.15
MITOCHONDRIAL MEMBRANE PART	50	1.02E-02	< 1.00E-04	2.01
MITOCHONDRION	300	8.56E-03	< 1.00E-04	1.99
MITOCHONDRIAL PART	132	3.86E-02	< 1.00E-04	1.90
SYNAPSE ORGANIZATION AND BIOGENESIS	18	8.90E-04	< 1.00E-04	-2.30
SYNAPTOGENESIS	15	4.45E-03	< 1.00E-04	-2.19
EXTRACELLULAR STRUCTURE ORGANIZATION AND BIOGENESIS	22	1.02E-02	< 1.00E-04	-2.08
***SMIT1* KO mice *vs.* WT-untreated mice**				
NAME	Size	FDR q-value	p-value	NES
STRUCTURAL CONSTITUENT OF RIBOSOME	77	< 1.00E-04	< 1.00E-04	2.69
RIBONUCLEOPROTEIN COMPLEX	121	< 1.00E-04	< 1.00E-04	2.35
RIBOSOME	35	< 1.00E-04	< 1.00E-04	2.34
ORGANELLAR RIBOSOME	21	1.93E-04	< 1.00E-04	2.23
MITOCHONDRIAL RIBOSOME	21	3.18E-04	< 1.00E-04	2.20
MITOCHONDRIAL MATRIX	42	2.11E-03	< 1.00E-04	2.12
MITOCHONDRIAL LUMEN	42	2.16E-03	< 1.00E-04	2.10
RIBOSOMAL SUBUNIT	19	2.10E-03	< 1.00E-04	2.09
MITOCHONDRIAL PART	130	5.68E-03	< 1.00E-04	2.02
MITOCHONDRIAL MEMBRANE PART	50	6.55E-03	< 1.00E-04	2.00
ACTIVE TRANSMEMBRANE TRANSPORTER ACTIVITY	78	2.32E-03	< 1.00E-04	-2.30
TRANSMEMBRANE RECEPTOR PROTEIN KINASE ACTIVITY	42	1.72E-03	< 1.00E-04	-2.24
RECEPTOR ACTIVITY	321	1.92E-03	< 1.00E-04	-2.19
PROTEIN TYROSINE KINASE ACTIVITY	46	1.44E-03	< 1.00E-04	-2.17
METALLOPEPTIDASE ACTIVITY	29	2.32E-03	< 1.00E-04	-2.14
TRANSMEMBRANE RECEPTOR PROTEIN TYROSINE KINASE ACTIVITY	34	1.94E-03	< 1.00E-04	-2.14
SECONDARY ACTIVE TRANSMEMBRANE TRANSPORTER ACTIVITY	27	3.17E-03	< 1.00E-04	-2.10
SUBSTRATE SPECIFIC TRANSPORTER ACTIVITY	246	3.20E-03	< 1.00E-04	-2.10
TRANSMEMBRANE TRANSPORTER ACTIVITY	232	4.42E-03	< 1.00E-04	-2.07
TRANSMEMBRANE RECEPTOR ACTIVITY	225	5.50E-03	< 1.00E-04	-2.05
SUBSTRATE SPECIFIC TRANSMEMBRANE TRANSPORTER ACTIVITY	216	5.21E-03	< 1.00E-04	-2.04
ION TRANSMEMBRANE TRANSPORTER ACTIVITY	167	7.01E-03	< 1.00E-04	-2.01
SYMPORTER ACTIVITY	16	7.54E-03	3.63E-03	-2.00
CATION TRANSMEMBRANE TRANSPORTER ACTIVITY	138	7.43E-03	< 1.00E-04	-2.00
CELL PROJECTION BIOGENESIS	20	1.24E-02	1.94E-03	-1.96
ANION TRANSMEMBRANE TRANSPORTER ACTIVITY	26	1.90E-02	< 1.00E-04	-1.92
MEMBRANE FRACTION	224	2.51E-02	< 1.00E-04	-1.89

* Size – number of genes included in a particular gene-set.

** FDR q-value – false discovery rate, adjusted to the gene-set size and multiple hypotheses testing

*** NES – normalized enrichment score (ES) Calculated by dividing the actual ES by the mean ES against all permutations performed. A positive score indicates up-regulation of the gene-set in KO mice as compared to WT-untreated mice. A negative score indicates down-regulation of the gene-set in KO mice as compared to WT-untreated mice.

Figure legends

Fig. S1: Schematic representation of the experiment design

A. The microarray part of the study. In green – animals, data and analyses related to the SMIT1 colony; in red – animals, data and analyses related to the IMPA1 colony; in black – analyses performed on the combined data obtained from both colonies.

B. The behavioral part of the study**.** Black arrows denote the beginning of rotenone (purple) and Li (blue) treatment. Colored arrows denote the behavioral experiments; red – rotarod and hanging wire tests, blue – FST, orange – amphetamine-induced hyperlocomotion.

Fig. S2: Statistical analysis of the raw data of the microarrays

Three-way mixed model ANOVA carried out to analyze the combined effect of lithium in both colonies revealed that the major source of variation between the groups was the colony. Type=treatment (Li or regular food), batch=random effect determined by principal component analysis (PCA), colony=IMPA1 or SMIT1.

Fig. S3: Hierarchal clustering of all genes differentially expressed in Li-treated mice from either of the colonies or in one of the KOs

Two-way ANOVA was carried out separately in each colony to reveal genes the expression of which was affected by Li treatment or KO of either *IMPA1* or *Slc5a3* as compared to WT-untreated mice. 4,643 genes differentially expressed ($p<0.05$) by either Li treatment or gene KO in either of the two colonies were used for the analysis. Signals from both colonies were used for the calculation of z-scores. The mice created two major clusters corresponding to the two colonies (IMPA1 and SMIT1). Highlighted in turquoise is the only gene cluster presenting similar expression pattern in the two colonies. Among the two sets of colored bars below the figure the upper represents the colony (blue – SMIT1, orange – IMPA1) and the lower - the type of mice (yellow – WT-untreated, pink – KO, grey – WT-Li treated).

Fig. S4: Functional annotation of the gene cluster showing similar expression pattern between the IMPA1 and SMIT1 colonies

Functional analysis of the gene cluster with similar expression between the two colonies (highlighted in turquoise in Fig. S2A) using DAVID software showed that

most of the functional annotations of the genes composing the cluster are related to mitochondrial respiration.

Fig. S5: DAVID Functional annotation tool reveals enrichment in mitochondria-related genes among genes with differential expression in KO mice and Li-treated mice in both SMIT1 and IMPA1 colonies

A list of significantly enriched terms ($p<0.05$, FDR<0.05) among genes with similar differential expression ($p<0.0.5$) in KO mice and Li-treated WT mice compared to WT-untreated mice.

A. Annotation clustering of 654 genes meeting the criteria in the SMIT1 colony.

B. Annotation clustering of 159 genes meeting the criteria in the IMPA1 colony.

Fig. S6: Ingenuity pathway analysis (IPA) shows great similarity between Li treatment, *IMPA1* KO and *Slc5a3* KO

We used the IPA software to compare canonical pathways and biological functions significantly affected in four groups of mice – *IMPA1* KO, *SMIT1* KO, Li-treated mice in the IMPA1 colony (IMPA_Li) and Li-treated mice in the SMIT1 colony (SMIT_Li).

A. Biological functions significantly affected by Li treatment and by *IMPA1* or *SMIT1* KO. Similarity is often more pronounced between Li treatment and KO in a given colony than between Li treatment in the two colonies.

B. The only three common canonical pathways significantly affected by Li treatment and by IMPA1 or SMIT1 KO were all related to mitochondrial function. The Y axes represent –log(p-value) of Fisher's exact test for the significance of the pathway/biological function. The red lines represent significance threshold corresponding to a p-value of 0.05.

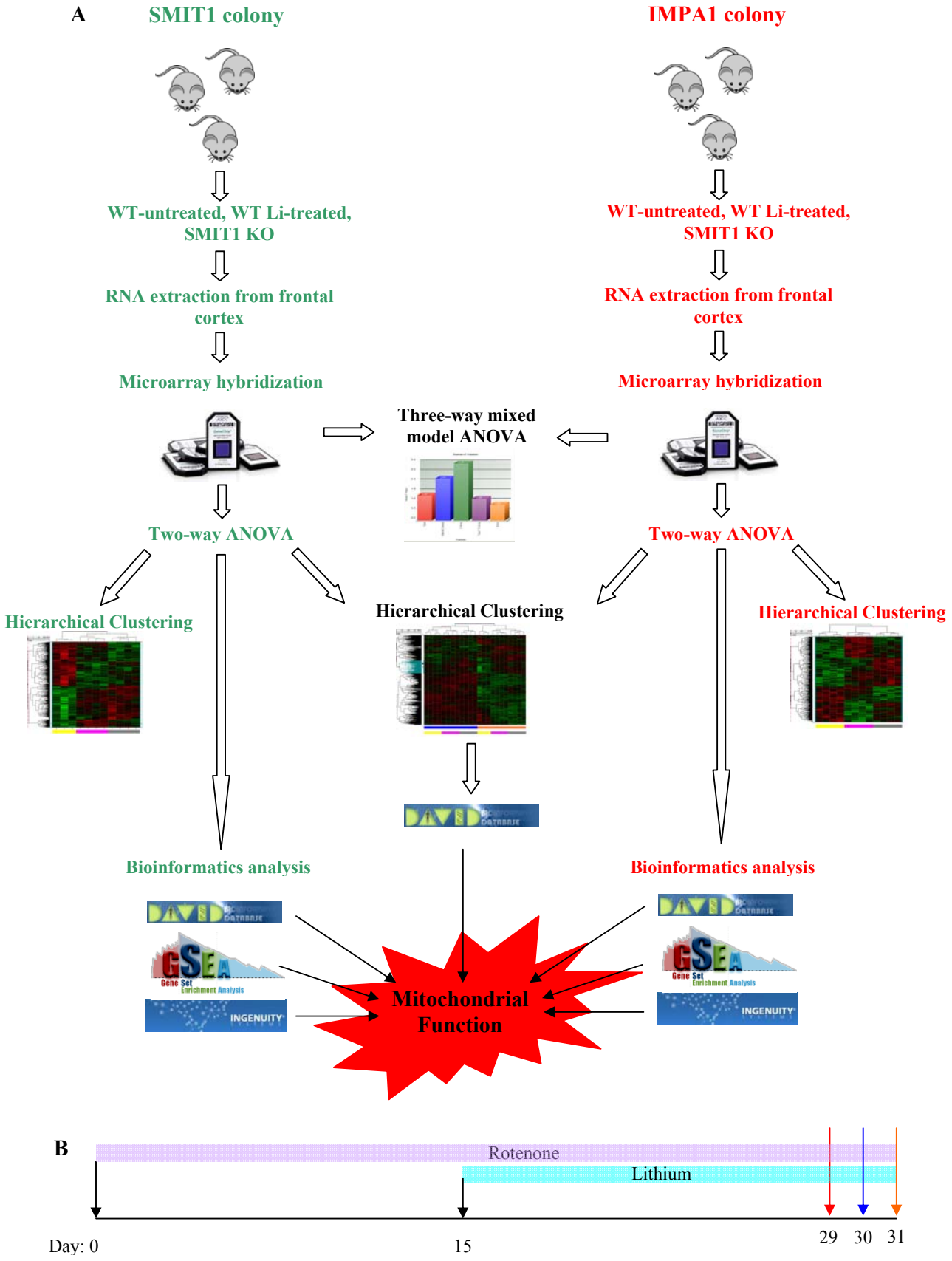

Fig. S1: Schematic representation of the study design

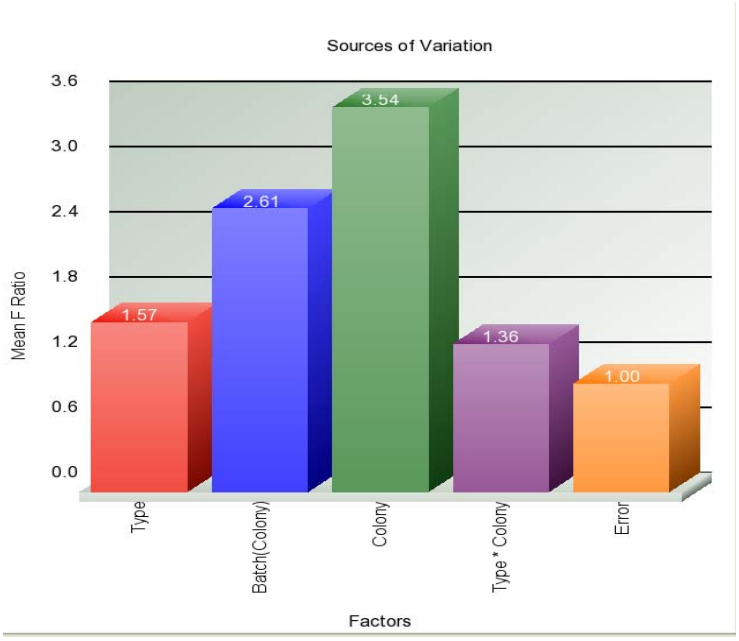

Fig. S2: Statistical analysis of the raw data of the microarrays

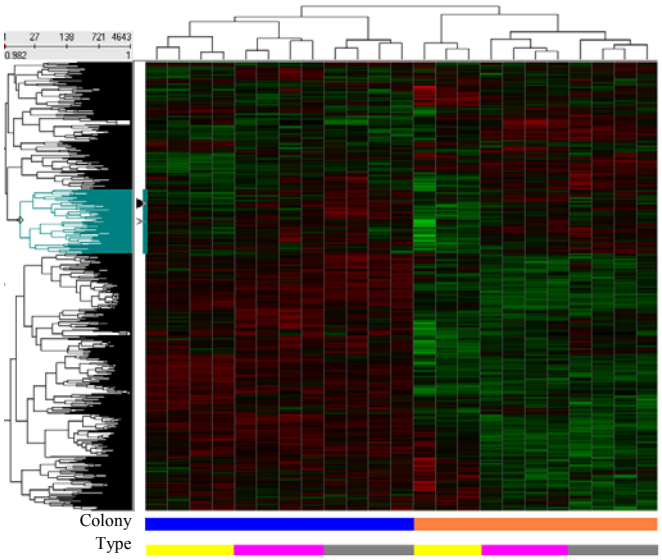

Fig. S3: Hierarchal clustering of all genes differentially expressed in Li-treated mice from either of the colonies or in one of the Kos

Category	Term	RT	Genes	Count	%	P-Value	Bonferroni	FDR
GOTERM_CC_FAT	mitochondrion	RT		85	20.3	9.3E-21	2.6E-18	1.2E-17
KEGG_PATHWAY	Parkinson's disease	RT		29	6.9	8.1E-20	8.7E-18	9.1E-17
GOTERM_CC_FAT	organelle inner membrane	RT		39	9.3	2.4E-18	6.6E-16	3.1E-15
GOTERM_CC_FAT	mitochondrial inner membrane	RT		38	9.1	2.9E-18	7.9E-16	3.8E-15
GOTERM_CC_FAT	organelle inner membrane	RT		39	9.3	2.4E-18	6.6E-16	3.1E-15
GOTERM_CC_FAT	mitochondrial inner membrane	RT		38	9.1	2.9E-18	7.9E-16	3.8E-15
KEGG_PATHWAY	Huntington's disease	RT		31	7.4	5.9E-18	6.3E-16	6.7E-15
KEGG_PATHWAY	Oxidative phosphorylation	RT		27	6.4	7.6E-18	8.1E-16	8.6E-15
GOTERM_CC_FAT	mitochondrial part	RT		49	11.7	8.0E-18	2.2E-15	1.1E-14
GOTERM_CC_FAT	mitochondrial membrane	RT		41	9.8	1.6E-17	4.5E-15	2.2E-14
GOTERM_CC_FAT	mitochondrial envelope	RT		42	10.0	2.3E-17	6.3E-15	3.0E-14
GOTERM_CC_FAT	respiratory chain	RT		19	4.5	1.3E-15	3.7E-13	1.8E-12
GOTERM_CC_FAT	organelle envelope	RT		46	11.0	4.0E-15	1.1E-12	5.3E-12
GOTERM_CC_FAT	envelope	RT		46	11.0	4.7E-15	1.3E-12	6.3E-12
KEGG_PATHWAY	Alzheimer's disease	RT		27	6.4	4.3E-14	4.7E-12	4.9E-11
GOTERM_CC_FAT	organelle membrane	RT		53	12.6	8.6E-13	2.4E-10	1.1E-9
GOTERM_BP_FAT	electron transport chain	RT		18	4.3	1.7E-10	2.3E-7	2.8E-7
GOTERM_BP_FAT	generation of precursor metabolites and energy	RT		26	6.2	2.6E-10	3.3E-7	4.2E-7
GOTERM_BP_FAT	translation	RT		28	6.7	7.7E-10	1.0E-6	1.3E-6
GOTERM_MF_FAT	hydrogen ion transmembrane transporter activity	RT		13	3.1	5.3E-8	2.2E-5	7.4E-5
GOTERM_CC_FAT	ribonucleoprotein complex	RT		31	7.4	7.6E-8	2.1E-5	1.0E-4
GOTERM_MF_FAT	monovalent inorganic cation transmembrane transporter activity	RT		13	3.1	1.0E-7	4.3E-5	1.5E-4
GOTERM_CC_FAT	ribosome	RT		18	4.3	9.3E-7	2.6E-4	1.2E-3
GOTERM_MF_FAT	oxidoreductase activity, acting on heme group of donors, oxygen as acceptor	RT		7	1.7	3.8E-6	1.6E-3	5.3E-3
GOTERM_MF_FAT	oxidoreductase activity, acting on heme group of donors	RT		7	1.7	3.8E-6	1.6E-3	5.3E-3
GOTERM_MF_FAT	cytochrome-c oxidase activity	RT		7	1.7	3.8E-6	1.6E-3	5.3E-3
GOTERM_MF_FAT	heme-copper terminal oxidase activity	RT		7	1.7	3.8E-6	1.6E-3	5.3E-3
GOTERM_MF_FAT	NADH dehydrogenase (ubiquinone) activity	RT		7	1.7	5.0E-6	2.1E-3	7.0E-3
GOTERM_MF_FAT	NADH dehydrogenase activity	RT		7	1.7	5.0E-6	2.1E-3	7.0E-3
GOTERM_MF_FAT	NADH dehydrogenase (quinone) activity	RT		7	1.7	5.0E-6	2.1E-3	7.0E-3
GOTERM_MF_FAT	inorganic cation transmembrane transporter activity	RT		13	3.1	6.4E-6	2.6E-3	8.9E-3
GOTERM_MF_FAT	structural constituent of ribosome	RT		14	3.3	7.3E-6	3.0E-3	1.0E-2
GOTERM_MF_FAT	oxidoreductase activity, acting on NADH or NADPH, quinone or similar compound as acceptor	RT		7	1.7	1.0E-5	4.3E-3	1.5E-2
GOTERM_CC_FAT	mitochondrial respiratory chain	RT		6	1.4	1.2E-5	3.2E-3	1.5E-2
GOTERM_MF_FAT	translation factor activity, nucleic acid binding	RT		11	2.6	1.9E-5	8.0E-3	2.7E-2
KEGG_PATHWAY	Ribosome	RT		11	2.6	3.9E-5	4.2E-3	4.4E-2

Fig. S4: Functional annotation of the gene cluster showing similar expression pattern between IMPA1 and SMIT1 colonies

A

Category	Term	RT	Genes	Count	%	P-Value	Fold Enrichment	Bonferroni	FDR
SP_PIR_KEYWORDS	acetylation	RT		152	23.2	6.6E-15	1.9	2.4E-12	9.0E-12
GOTERM_CC_FAT	mitochondrion	RT		94	14.4	1.2E-11	2.0	4.1E-9	1.6E-8
GOTERM_CC_FAT	mitochondrial part	RT		49	7.5	1.2E-9	2.6	4.2E-7	1.6E-6
SP_PIR_KEYWORDS	mitochondrion	RT		63	9.6	1.5E-9	2.3	5.5E-7	2.1E-6
GOTERM_CC_FAT	organelle membrane	RT		64	9.8	2.4E-9	2.2	8.4E-7	3.3E-6
KEGG_PATHWAY	Parkinson's disease	RT		21	3.2	1.1E-8	4.7	1.4E-6	1.3E-5
GOTERM_CC_FAT	mitochondrial membrane	RT		38	5.8	1.0E-8	2.9	3.6E-6	1.4E-5
SP_PIR_KEYWORDS	phosphoprotein	RT		288	44.0	1.2E-8	1.3	4.5E-6	1.7E-5
KEGG_PATHWAY	Huntington's disease	RT		24	3.7	4.2E-8	3.8	5.7E-6	5.0E-5
GOTERM_CC_FAT	mitochondrial envelope	RT		38	5.8	4.8E-8	2.7	1.7E-5	6.6E-5
GOTERM_CC_FAT	mitochondrial inner membrane	RT		32	4.9	6.5E-8	3.0	2.3E-5	8.9E-5
KEGG_PATHWAY	Oxidative phosphorylation	RT		20	3.1	7.9E-8	4.4	1.1E-5	9.2E-5
SP_PIR_KEYWORDS	mitochondrion inner membrane	RT		24	3.7	1.0E-7	3.8	3.7E-5	1.4E-4
SP_PIR_KEYWORDS	respiratory chain	RT		14	2.1	1.5E-7	6.5	5.3E-5	2.0E-4
GOTERM_CC_FAT	organelle inner membrane	RT		32	4.9	2.2E-7	2.9	7.6E-5	3.0E-4
GOTERM_BP_FAT	electron transport chain	RT		17	2.6	1.1E-6	4.5	1.9E-3	1.8E-3
GOTERM_CC_FAT	respiratory chain	RT		13	2.0	2.3E-6	5.7	7.9E-4	3.1E-3
GOTERM_CC_FAT	organelle envelope	RT		41	6.3	7.9E-6	2.1	2.8E-3	1.1E-2
GOTERM_CC_FAT	envelope	RT		41	6.3	8.7E-6	2.1	3.0E-3	1.2E-2
SP_PIR_KEYWORDS	electron transport	RT		15	2.3	8.7E-6	4.3	3.1E-3	1.2E-2
GOTERM_BP_FAT	generation of precursor metabolites and energy	RT		25	3.8	8.5E-6	2.8	1.5E-2	1.4E-2

B

Sublist	Category	Term	RT	Genes	Count	%	P-Value	Bonferroni	FDR
☑	KEGG_PATHWAY	Oxidative phosphorylation	RT		13	8.2	2.1E-9	1.2E-7	2.1E-6
☑	KEGG_PATHWAY	Parkinson's disease	RT		12	7.5	3.4E-8	1.9E-6	3.4E-5
☑	KEGG_PATHWAY	Huntington's disease	RT		13	8.2	1.0E-7	5.7E-6	1.0E-4
☑	SP_PIR_KEYWORDS	mitochondrion inner membrane	RT		12	7.5	3.0E-7	6.1E-5	3.8E-4
☑	SP_PIR_KEYWORDS	mitochondrion	RT		23	14.5	4.1E-7	8.5E-5	5.2E-4
☑	KEGG_PATHWAY	Alzheimer's disease	RT		12	7.5	8.6E-7	4.8E-5	8.5E-4
☑	GOTERM_CC_FAT	organelle envelope	RT		18	11.3	2.4E-6	4.8E-4	3.0E-3
☑	GOTERM_CC_FAT	envelope	RT		18	11.3	2.5E-6	5.0E-4	3.1E-3
☑	GOTERM_CC_FAT	mitochondrial envelope	RT		15	9.4	4.7E-6	9.5E-4	5.9E-3
☑	SP_PIR_KEYWORDS	transit peptide	RT		16	10.1	4.8E-6	9.8E-4	6.0E-3
☑	GOTERM_CC_FAT	mitochondrial inner membrane	RT		13	8.2	6.8E-6	1.4E-3	8.5E-3
☑	SP_PIR_KEYWORDS	respiratory chain	RT		7	4.4	1.1E-5	2.2E-3	1.4E-2
☑	UP_SEQ_FEATURE	transit peptide:Mitochondrion	RT		16	10.1	9.9E-6	4.7E-3	1.4E-2
☑	GOTERM_CC_FAT	organelle inner membrane	RT		13	8.2	1.2E-5	2.3E-3	1.5E-2
☑	GOTERM_CC_FAT	mitochondrial membrane	RT		14	8.8	1.2E-5	2.5E-3	1.5E-2
☑	GOTERM_CC_FAT	respiratory chain	RT		7	4.4	1.7E-5	3.4E-3	2.1E-2
☑	GOTERM_CC_FAT	mitochondrial part	RT		16	10.1	3.0E-5	6.1E-3	3.8E-2

Fig. S5: DAVID Functional annotation tool reveals enrichment in mitochondria-related genes among genes with differential expression in KO mice and Li-treated mice in both colonies

A

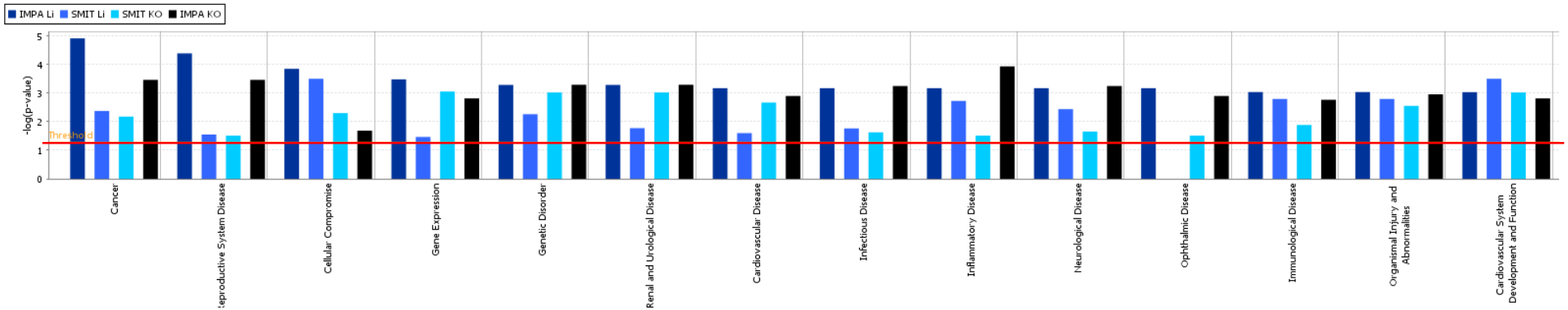

B

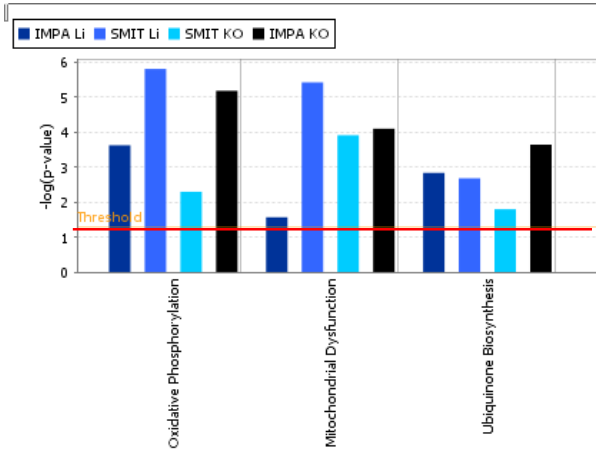

Fig. S6: Ingenuity Pathway Analysis shows great similarity between Li treatment, *IMPA1* KO and *Slc5a3* KO